

Supplementary Materials

The PDF file includes:

Materials and Methods

Fig. S1. Trametinib decreases cell viability in RAS-mutated RMS in vitro.

Fig. S2. Trametinib induces G1 arrest and differentiation in RAS-mutated RMS.

Fig. S3. ERK2 is associated with developmental gene regulation in RAS-mutated cancer cell lines.

Fig. S4. MYOG associates with opened chromatin in trametinib-treated RMS cells.

Fig. S5. Super-enhancers in RAS-mutated RMS cell lines correlate with super-enhancers in RAS-mutated RMS tumors.

Fig. S6. RAS-dependent super-enhancers are not observed in human skeletal muscle myoblasts.

Fig. S7. MEK inhibition delays tumor growth in RD xenografts.

Fig. S8. Combination of trametinib and BMS-754807 delays tumor growth in RD xenografts.

Fig. S9. MEK inhibition induces transcriptional reprogramming analogous to myogenic differentiation in FN-RMS.

References (77–89)

Other Supplementary Material for this manuscript includes the following:

(available at www.sciencetranslationalmedicine.org/cgi/content/full/10/448/ean4470/DC1)

Table S1 (Microsoft Excel format). Dose response as %AUC for RMS and normal cell lines.

Table S2 (Microsoft Excel format). Differentially expressed genes in SMS-CTR treated with trametinib or SCH772984.

Table S3 (Microsoft Excel format). Differentially expressed genes in RD treated with trametinib or MEK1 siRNA SMS-CTR.

Table S4 (Microsoft Excel format). GSEA SMS-CTR treated with trametinib.
Table S5 (Microsoft Excel format). GSEA RD treated with trametinib.
Table S6 (Microsoft Excel format). HSMMdiff_UP gene set.
Table S7 (Microsoft Excel format). ERK2 ChIP-seq peaks.
Table S8 (Microsoft Excel format). Trametinib-changed DNase-seq peaks.
Table S9 (Microsoft Excel format). MYOD, MYC, and MYOG peaks in SMS-CTR treated with trametinib.
Table S10 (Microsoft Excel format). Super-enhancers with and without trametinib.
Table S11 (Microsoft Excel format). Gene Expression Omnibus data sets used in this analysis.
Table S12 (Microsoft Excel format). STR genotyping of RMS cell lines used in this study.
Table S13 (Microsoft Excel format). Primers used in this study.
Table S14 (Microsoft Excel format). Vectors used in this study.
Table S15 (Microsoft Excel format). Antibodies used in this study.
Table S16 (Microsoft Excel format). RAS-dependent_SE_DOWN and Myogenic_SE_UP gene sets.
Table S17 (Microsoft Excel format). Pilot 6×6 matrix screen excess HSA.
Table S18 (Microsoft Excel format). Matrix screen (10×10) excess HSA.

Materials and Methods

Cell Lines, Plasmids and Compounds

Cell lines were obtained as previously described (51). All cell lines were confirmed to be mycoplasma negative using the MycoAlert kit (Lonza) and unique by STR DNA fingerprinting prior to experimental use (supplemental table 12). RD, SMS-CTR, CCA, HEK293T, NIH3T3, X7250, Rh41, RH5, Rh30, NCIARMS, JR1, and C2C12 cells were grown in high glucose Dulbecco Modified Eagle Medium (DMEM, Quality Biological) with 10% Fetal Bovine Serum (FBS, Life Technologies). BIRCH cells were grown in Roswell Park Memorial Institute medium (RPMI, Quality Biological) with 10% FBS. RMS559 cells were grown in Iscove Modified Dulbecco medium (IMDM, Quality Biological) with 15% FBS. Published siRNAs for HRAS, NRAS (77) and no known human gene were cloned into PLKO.1 (Addgene) to create shRNAs (sequences available in supplemental table 13). Expression constructs for HRAS Q61L, KRAS G12V, NRAS Q61K, BRAF V600E, myr-AKT, and RALA-Q75L in pBABE were purchased from Addgene as indicated in supplemental table 14. An expression construct for MYOG-HA was also purchased from Addgene and subcloned into pBABE.

For pBABE-containing retrovirus production, 1 million HEK293T cells were plated in 6 cm dishes 24 hours prior to transfection with both 1 μ g of the desired pBABE vector and 1 μ g of pCL-10A1 using Lipofectamine 2000 (Life technologies). Viral supernatants were harvested at 48 and 72 hours after transfection for direct transduction of RD or C2C12 cells in the presence of 8 μ g/mL polybrene (Sigma). 24 hours following the second transduction, the RD or C2C12 cells were split into selection with 2 μ g/mL puromycin or 400 μ g/mL Zeocin (BRAF only).

For PLKO.1 containing lentivirus production, 1 million HEK293T cells were plated in 6 cm dishes for 24 hours prior to transfection with shRNA containing PLKO.1, psPAX2 and pMD2.G at a 4:3:1 ratio with Lipofectamine 2000. Resulting lentiviral particles were harvested 48 and 72 hours post-transfection and pooled. 1 mL of each viral containing suspension was used to transduce RD or SMS-CTR cells plated in T25 flasks in the presence of 8 μ g/mL polybrene. 48 hours following transduction, the RD or SMS-CTR cells were split into selection with 2 μ g/mL puromycin.

Commercial siRNAs (MAP2K1, Silencer select negative control #2, and AllStars cell death control) were purchased from Qiagen or Life Technologies and reverse transfected into cells using RNAimax (Life Technologies). Trametinib, BMS-754807, palbociclib, and SCH-772984 were obtained from the NIH Developmental Therapeutics Program (DTP). Vx11e and ulixertinib were obtained from SelleckChem.

DNA content analysis

Cells were fixed with 70% ethanol prior to staining with propidium iodide/TritonX-100. Stained cells were analyzed using a FACS Calibur instrument (BD Biosciences) with 488 nm excitation. Cell cycle analysis was performed in ModFit LT version 5 using default parameters.

Immunoblot experiments

Antibodies used in this study are listed in supplemental table 15. Cells in culture were washed twice with ice cold PBS prior to lysis in mammalian protein extraction reagent (MPER) with added HALT protease and phosphatase inhibitors (Thermo). Cells were lysed at 4 °C for 10 minutes prior to disruption with syringe and 20-gauge needle. Lysates were clarified by centrifugation at 16,000 rpm at 4 °C for 10 minutes. Protein concentration of the resulting supernatant was estimated by BCA assay. 10-40 µg of sample were run on NuPage 4-12% BisTris minigels (Novex) and transferred to PVDF membranes using the iBlot (Life Technologies). Membranes were blocked in 5% nonfat dried milk in TBST for 1 hour at room temperature and incubated with primary antibodies overnight at 4 °C. HRP-conjugated anti-rabbit or mouse antibodies (CST) were used as secondary antibodies, as indicated in supplemental table 15. Protein was visualized using SuperSignal West Dura or Femto (Thermo). Tissue lysates were prepared by pulverizing fresh frozen tumor tissue in a BioPulverizer prior to dissolving the resulting powder in TPER buffer (Thermo).

Xenograft experiments

Xenograft studies were approved by the Animal Care and Use Committee of the NCI-Bethesda (trametinib alone) or the NCI-Frederick (combination), and all animal care was in accordance with institutional guidelines. The NOG-F homozygous/homozygous NOD.Cg-*Prkdc*^{scid} *Il2rg*^{tm1Sug}/JicTac (NOG) mice used in these experiments were purchased from Taconic Bioscience and bred as a local colony in our laboratory. The Fox Chase SCID Beige Mouse CB17.B6-*Prkdc*^{scid}Lyst bg/Crl (SCID Beige) mice were purchased from Charles River laboratories. All animals were female and all were injected at 4-8 weeks of age. For the SMS-CTR trametinib monotherapy experiments, 2 or 5 million cells were injected orthotopically into the gastrocnemius muscle in the left hind leg of 8 NOG mice. After 3 weeks, the mice were randomized into vehicle and trametinib groups of 4 mice each (equivalent tumor size in each group). Trametinib suspensions were prepared in vehicle (0.5% hydroxypropylmethylcellulose/0.2% Tween 80/5% sucrose) weekly and stored at 4 °C until use. The treatment group mice received trametinib at a dose of 3 mg/kg (100 µL of a 0.3 mg/mL suspension) by oral gavage daily (78); the vehicle group received the same volume of vehicle by oral gavage daily.

In the BIRCH experiments, NOG mice were injected orthotopically with 5 million cells as described above. Mice were randomized into vehicle (3 mice) or trametinib (5 mice) groups 3 weeks after cell injection, and were treated as described above. In the RD experiments, SCID Beige mice were injected orthotopically with 2 million cells as described above. Mice were randomized into vehicle (10 mice) or trametinib (10 mice) groups 3 weeks after cell injection and were treated as described above.

In the combination experiments, SCID Beige mice were injected with 2 million RD or SMS-CTR cells orthotopically as above. After 3 weeks, mice were randomized into 4 groups of 10 mice each (vehicle, trametinib alone, BMS-754807 alone, or combination). Trametinib was prepared as above and administered by oral gavage on Monday through Friday in the morning. BMS-754807 was prepared in a vehicle of PEG 400: sterile water at a ratio of 80:20 and administered by oral gavage on Monday through Friday in the afternoon at a dose of 50 mg/kg (100 µL of a 5 mg/mL solution) (79). Mice were treated for a 28-day cycle, given a 7-day rest,

and then treated for an additional 2 weeks, at which time all the vehicle mice had reached tumor endpoint. For tumor shrinkage experiments, mice were injected with RD, SMS-CTR or BIRCH as above, and tumors were allowed to grow to 1000 mm³ prior to initiation of treatment (5 mice per treatment group per cell line). Tumors were harvested from 2 mice per group after 5 days of treatment, 3 hours after the last dose of trametinib or vehicle for immunoblot, capillary immunoassay or immunohistochemistry experiments. The remaining animals were monitored for tumor response.

In all experiments, the leg dimensions were measured twice a week with digital calipers to obtain two diameters of the tumor sphere, from which the tumor volume was determined using the equation $(D \times d^2)/6 \times 3.14$ (where D = the maximum diameter and d = the minimum diameter) (80). Animals were euthanized when they reached tumor endpoint, which was defined as when the tumor measured greater than 2 cm in any direction, showed signs of ulceration, or caused significant discomfort to the animal, in accordance with the humane endpoints recommended by our institutional Animal Care and Use Committee (ACUC). The log-rank (Mantel-Cox) test was used to compare event-free survival distributions between treatment groups. Tumor doubling time was determined by fitting the tumor volume versus time curve for the vehicle treated animals to an exponential growth equation.

Immunohistochemistry experiments

Tumor tissue was fixed in formalin and tissue blocks were prepared by embedding the fixed tissue in paraffin. Antigen retrieval was performed with citrate buffer for 10 minutes at 100 °C. Sections were cooled, and IHC staining was carried out using the Mouse on Mouse (M.O.M.) ImmPRESS HRP Polymer Kit (Vector Laboratories #MP-2400) and myogenin antibody (Invitrogen Life Technologies #MA1-41042), diluted 1:50, for 30 minutes. Isotype control reagent was used in place of the myogenin antibody as a negative control. Slides were digitized with an Aperio ScanScope XT (Leica) at 200X in a single z-plane. Aperio whole-slide images were evaluated and graded for staining intensity by a board-certified veterinary pathologist (EFE). Images of the entire tumor section were manually segmented to exclude regions of intratumoral necrosis and of stroma surrounding the tumor, and automated algorithms were run to assess the positive cells as % total nuclei in the segmented region.

Capillary Immunoassays

Cell lysates were prepared in MPER (Thermo). Fresh frozen tumor samples were pulverized using a Biopulverizer mortar and pestle and then dissolved in TPER (Thermo). Cell or tumor lysates were mixed with 1x sodium dodecyl sulfate master mix containing sample buffer (ProteinSimple, catalog # 042-195), dithiothreitol, and fluorescently labeled standards (ProteinSimple, catalog # PS-ST01) and were heated at 70 °C for 10 minutes before being loaded into Peggy Sue instrument for analysis. During electrophoresis, proteins were separated by molecular weight while migrating through the separation matrix (ProteinSimple, catalog# 042-512). Separated proteins were immobilized on the capillary wall using UV light, and incubated with a blocking reagent (ProteinSimple, catalog # 042-514), followed by immunoprobings with respective primary antibodies and HRP conjugated anti-rabbit or anti-mouse secondary antibodies (ProteinSimple catalog# 042-206, Jackson ImmunoResearch catalog# 111-035-144 or

715-035-150). A 1:1 mixture of luminol and peroxide (ProteinSimple catalog# 043-311 and 043-379 respectively) was added to generate chemiluminescence, which was captured by a CCD camera. The digital image was analyzed by Compass software (ProteinSimple). Target protein quantities were determined by quantifying the signal strength (peak area). The Simple Western total protein assay was employed as a loading control. In the total protein analysis module, proteins were separated by MW and immobilized in the capillary, prior to incubation with biotinylating reagent (ProteinSimple, catalog # 042-973 & 042-975), followed by HPR-streptavidin (ProteinSimple, catalog # 042-976) for chemiluminescent detection.

RT-qPCR experiments

Quantitative RT-PCR was performed using Taqman assays (supplemental table 13, Life Technologies). Briefly, cDNA was generated from 200 ng of RNA using reverse transcription. Then PCR was carried out in a 96-well plate using a Viia 7 real-time PCR system (Life Technologies). Triplicates were performed for each gene for every sample, and average threshold cycle (C_t) numbers were calculated. Gene expression levels were represented by normalized C_t ($-\Delta C_t$) against GAPDH.

RNA-seq experiments

RNA was extracted using the RNeasy mini kit (Qiagen). Poly-A selected RNA libraries were prepared and sequenced on an Illumina HiSeq2000. QC was performed using FastQC version 0.11.2 and Picard's version 1.127 RNASEqMetrics function with the default parameters. PCR duplicates were marked using Picard's MarkDuplicates function, also from Picard version 1.127. Coverage was determined using bedtools version 2.22.0. RNA-seq reads were aligned to the UCSC hg19 reference genome using TopHat version 2.0.13 with parameters --keep-fastq-order, --no-coverage-search, --fusion-search, --fusion-min-dist 100000, --mate-inner-dist 84, and --mate-std-dev 74. Cufflinks version 2.2.1 was called with the following altered parameters: --no-update-check --max-bundle-frags 8000000000000 --max-bundle-length 10000000 to estimate transcript abundance levels. Cuffdiff (part of cufflinks version 2.2.1) was run with default parameters to find significant differences in transcript expression. Significance was defined as having FDR q-value <0.01 and FWER p-value of <0.05. Gene set enrichment analysis (<http://www.broadinstitute.org/gsea/index.jsp>) was performed using default parameter settings.

ChIP-seq

Chromatin immunoprecipitations were performed on C2C12 myoblasts, RMS cell lines, and RMS tumor tissue using the ChIP-IT High sensitivity kit (Active Motif). Antibodies used are detailed in Table S15. Resultant purified immunoprecipitated DNA was used for qPCR (Viia 7, Life Technologies) or for library preparation using the TruSeq ChIP sample preparation kit (Illumina) without modifications. 11-18 library preps were mixed for multiplexed single read sequencing using the NextSeq500 (Illumina). Reads were aligned to the hg19 reference using BWA (version 0.7.10), with a read mapping quality threshold set to $q = 30$. ChIP-seq peaks were identified using MACS 2.1 (81), using the callpeak function, parameters = [--format BAM -control input.bam --keep-dup all --pvalue 0.00001]. Motif finding was performed using Homer v4.2 (82), utilizing findMotifsGenome.pl (coordinates given as bed format ChIP-seq peaks

identified with MACS2) with [-size 1000 -len 10 -p 32]. Gene ontology was performed using GREAT (39), using hg19 and the whole genome as the background. Chromatin states were characterized using ChromHMM (83) using the LearnModel function set to 14 states. Enhancers were identified and rank-ordered using ROSE2 (<https://github.com/linlabbcm/rose2>) and standard definitions of super and typical enhancers (84), where the threshold is set to the inflection point of acetylation ChIP-seq signal among ranked enhancers. Differential peak calling between DMSO and trametinib treated samples was performed using BEDTools v2.25.0 (85) in multicov mode to measure read counts, which were normalized per million mapped reads, and visualized using R package ggplot2 or NGS plot (86). Genomic regions were visualized using IGV v2.3.40. Core regulatory transcription factor circuitry analysis was performed using COLTRON (53), with each super enhancer being assigned to a transcription factor if expressed at an FPKM of at least 4, and no farther than 1,500 Kb. Regulatory networks were visualized with R package qgraph, where the size of the nodes were set to $\log_2(\text{FPKM})$ and the edges were given as arrows from any transcription factors whose motif was present in the super enhancer assigned to the target transcription factor node. Enhancer regions were linked to their nearest gene, irrespective of strand specificity and gene direction, within topologically associated domain (TAD) boundaries using EDEN (51). For ERK2 and RNA Pol II ChIP-seq, 40 ng exogenous *Drosophila* chromatin (Active Motif, catalogue no. 53083) was used to spike-in normalize for global changes in binding by simultaneously performing ChIP with the *Drosophila* specific H2Av antibody (Active Motif, catalogue no. 61686). Reference genome normalization (RRPM, reference-adjusted reads per million mapped reads) was calculated with the ChIP-Rx method (87). The source of tumor tissue has been previously described (88).

Clustering of cell lines and tumors with epigenetic SE signatures

A master set of super enhancer regions found in 41 H3K27ac datasets was generated from the union of super enhancers regions identified in each sample. Overlapping super enhancers were merged into a single region. Read coverage in every super enhancer for each sample was calculated using bedtools multicov (85), and a pairwise Pearson correlation matrix was generated from ChIP-seq signal vectors of reads per million mapped reads normalized for region size. Complete-linkage hierarchical clustering was performed followed by visualization with heatmap.2 in R package gplots (<https://cran.r-project.org/web/packages/gplots/gplots.pdf>). Public data used in this comparative super enhancer analysis were downloaded from Gene Expression Omnibus (GEO), for which series numbers and SRA accession numbers have been listed in Supplemental Table 11.

DNase-seq

Genome wide DNase I hypersensitive sites were identified essentially as described (89) with slight modification. In brief, ten thousand SMS-CTR cells treated for 48 hours with either DMSO or 100 nM trametinib were lysed for 1 minute at room temperature in RSB lysis buffer. Lysed cells were then incubated with DNase I (Roche) at 37 degrees C for 5 min. DNA was purified using the MiniElute PCR purification kit (Qiagen). Libraries were prepared using the TruSeq ChIP sample preparation kit and sequenced using multiplexed paired-end sequencing on a NextSeq 500 (Illumina). Data analysis was performed per the ChIP-seq pipeline described above. For determination of regions of increased and decreased chromatin accessibility as a

function of trametinib treatment, DNase hypersensitivity peaks were defined as those with less than 5-fold difference in peak intensity between two replicates. Trametinib increased regions were defined as the peaks for which there was an increase greater than 5 RPM (reads per million mapped reads across all DNase regions) in peak intensity in the presence of trametinib. Conversely, trametinib decreased regions were defined as the peaks for which there was a greater than 5 RPM decrease in peak intensity in the presence of trametinib. DNase hypersensitivity peaks were linked to their nearest gene as described for enhancers above.

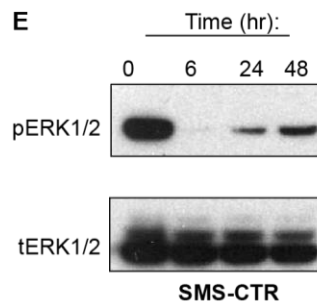
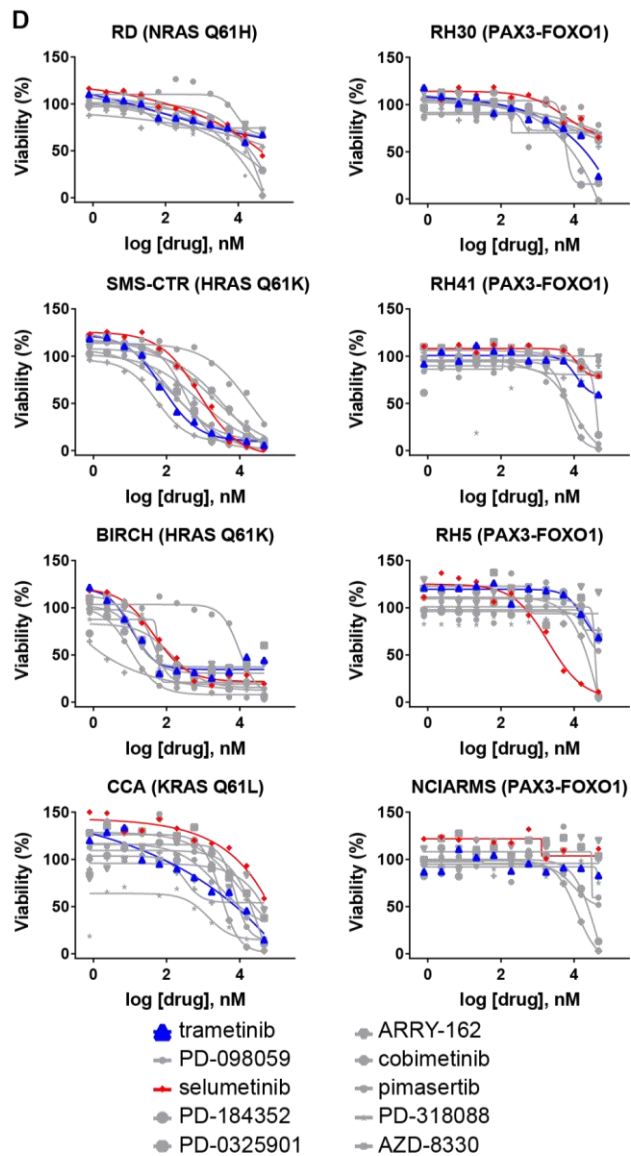
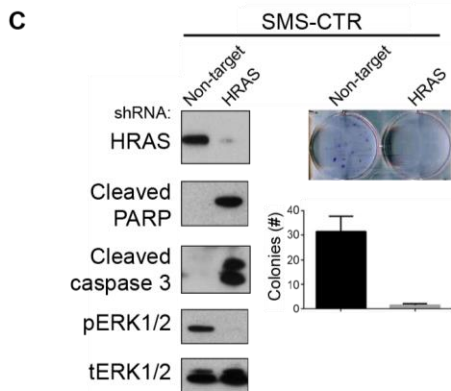
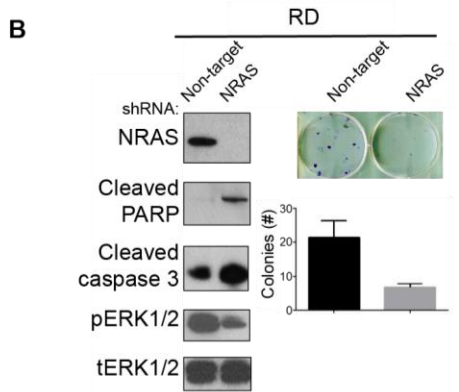
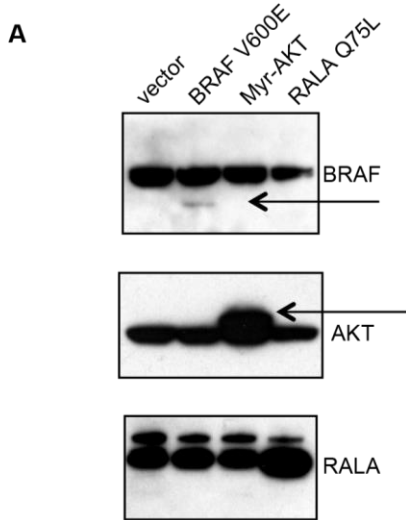


Fig. S1. Trametinib decreases cell viability in RAS-mutated RMS in vitro. (A) Stable expression of RAS effectors in C2C12 cells is confirmed by immunoblot. Arrows denote bands corresponding to FLAG-tagged versions of BRAF and AKT. The wild type protein is the main band observed. (B) shRNA-mediated knock-down of NRAS expression in the RD cell line (*NRAS* Q61H) induces PARP and caspase 3 cleavage, and decreases ERK phosphorylation, as determined by immunoblot (left). In addition, knock-down of NRAS expression in this cell line decreases proliferation, as determined by a 14-day clonogenic assay (right). Data are represented as mean \pm SD for 3 experiments. (C) shRNA-mediated knock-down of HRAS expression in the CTR cell line (*HRAS* Q61K) also induces expression of apoptotic markers, decreases ERK phosphorylation (left) and decreases cell proliferation (right). (D) Cell viability dose response curves for 10 MEK inhibitors in 4 RAS-mutated FN-RMS cell lines, RD, SMS-CTR, BIRCH, and CCA, and in 4 FP-RMS cell lines, RH30, RH41, RH5, and NCIARMS. (E) The decrease in ERK phosphorylation in SMS-CTR cells treated with trametinib is transient, as determined by immunoblot.

Figure S2

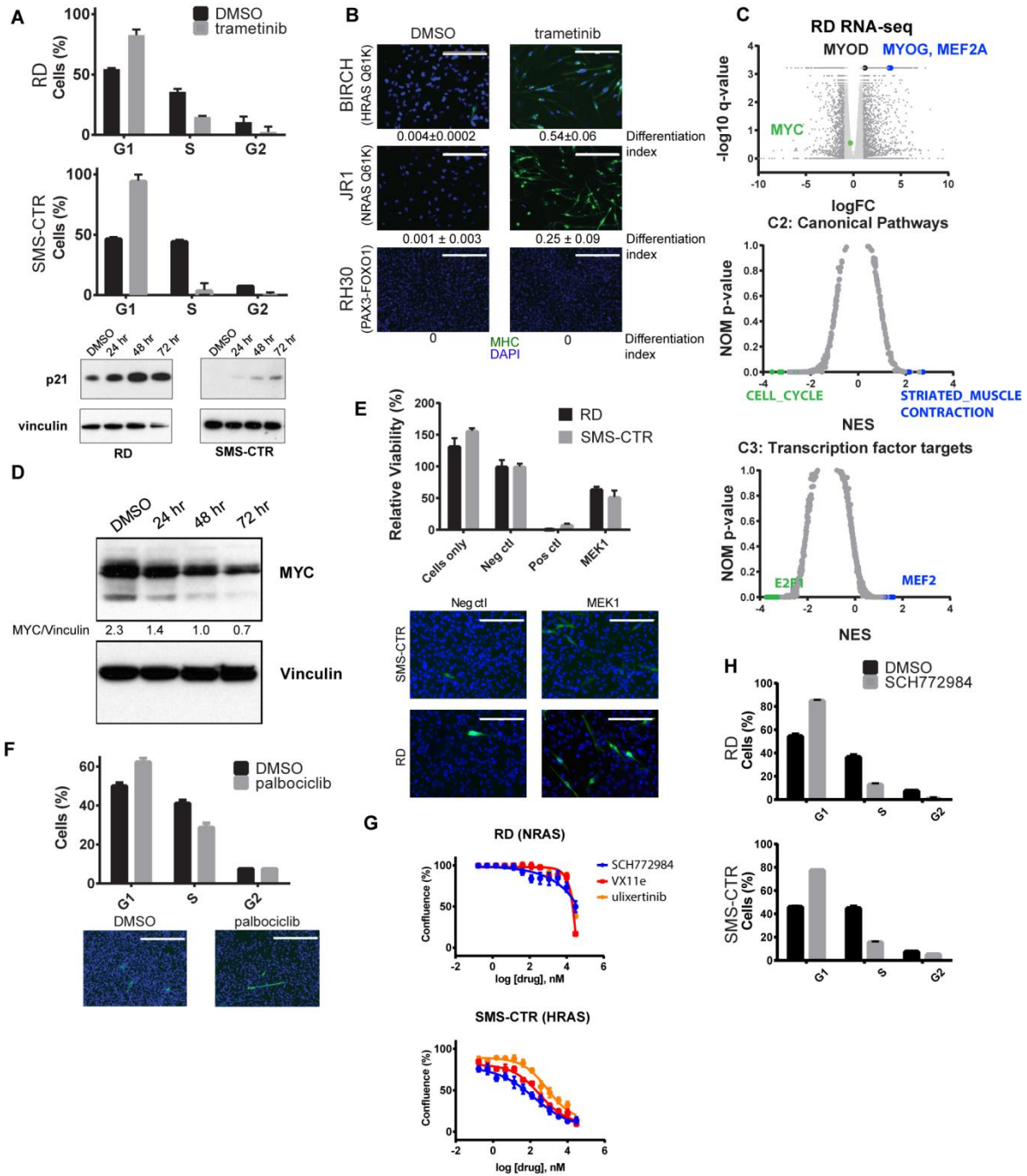
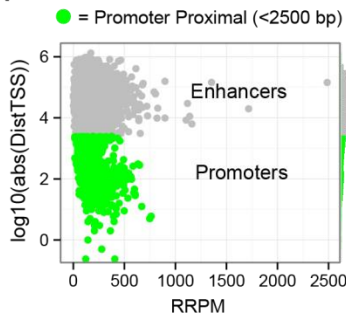


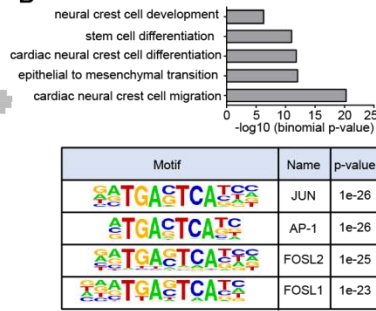
Fig. S2. Trametinib induces G1 arrest and differentiation in RAS-mutated RMS. (A)

Treatment with 100 nM trametinib for 48 hours induces G1 arrest in RD (top) and SMS-CTR (bottom) as determined by DNA content analysis. **(B)** Trametinib treatment for 72 hours induces differentiation in two additional FN-RMS cell lines (BIRCH and JR1), but not RH30 (FP-RMS), as determined by immunofluorescent staining of MHC. **(C)** Volcano plot comparing gene expression in RD treated with 100 nM trametinib for 48 hours with RD treated with vehicle for 48 hours (top). Statistically significant differentially expressed genes (at least 2-fold change with $p < 0.05$) are represented by dark gray dots; genes that are not differentially expressed are represented by light gray dots. Significance (nominal p-value) versus normalized enrichment score (NES) plot for gene sets in the C2: canonical pathways molecular signatures database (center) or C3: transcription factor motif molecular signatures database (bottom) are also shown. **(D)** Expression of *MYC* is decreased by trametinib treatment in RD, as determined by immunoblot. **(E)** RD and SMS-CTR were reverse transfected in 96-well plates with no siRNA (cells only), negative control siRNA (silencer select negative control #2), positive control siRNA (AllStars Cell Death control), or siRNA specific for MEK1 (*MAP2K1*). Cell viability was determined by CellTiter Glo 72 hours after siRNA transfection. Data are represented as mean \pm SD (top). In addition, RD and SMS-CTR were reverse transfected in 6-well plates with negative control siRNA or MEK1-specific siRNA. Transfected cells were grown in complete medium for 72 hours before determination of MHC expression by immunofluorescence (bottom). Scale bars correspond to 400 μm . **(F)** G1 arrest is induced in SMS-CTR treated for 72 hours with 100 nM palbociclib, a CDK4/6 inhibitor, as determined by DNA content analysis (top). Data are represented as mean \pm SD. No induction of MHC expression was detected by immunofluorescence in SMS-CTR treated with 100 nM palbociclib for 72 hours in complete medium (bottom). Scale bars indicate 400 μm . **(G)** Cell viability dose response curves for 3 ERK inhibitors in RD and SMS-CTR. **(H)** Treatment with 100 nM SCH772984 for 48 hours induces G1 arrest in RD (top) and SMS-CTR (bottom) as determined by DNA content analysis.

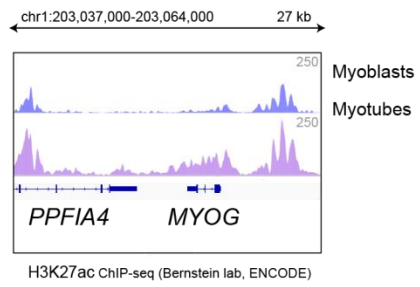
A ERK2 Genomic Distribution



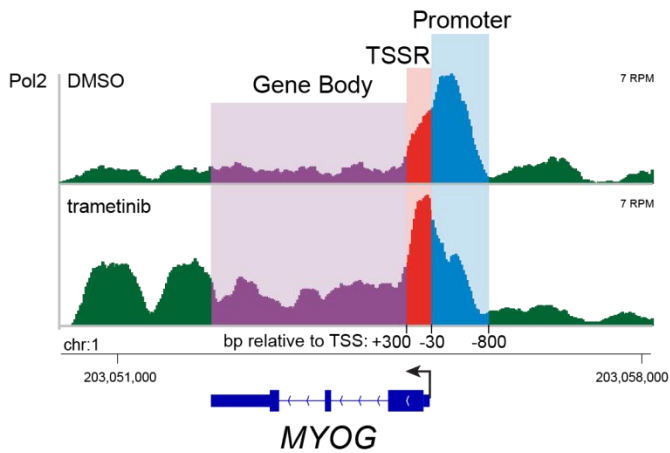
B ERK2 sites in Neuroblastoma (SK-N-AS)



C

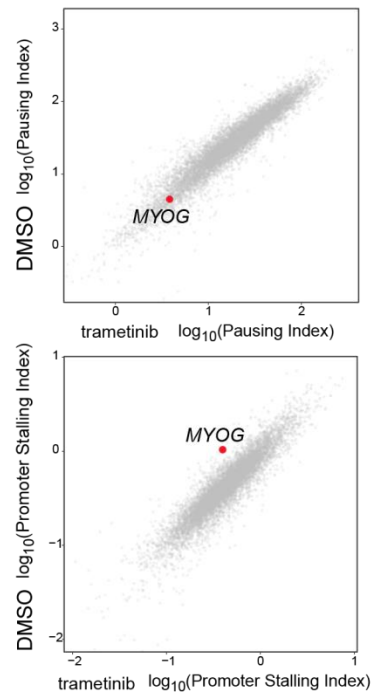


D

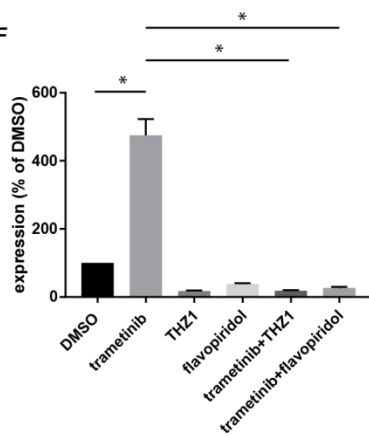


	DMSO	trametinib
Pausing Index (Traveling Ratio) = $\frac{\text{Pol2 TSSR Density}}{\text{Pol2 Gene Body Density}}$	4.48	3.82
Promoter Stalling Index = $\frac{\text{Pol2 Promoter Density}}{\text{Pol2 TSSR Density}}$	1.04	0.40

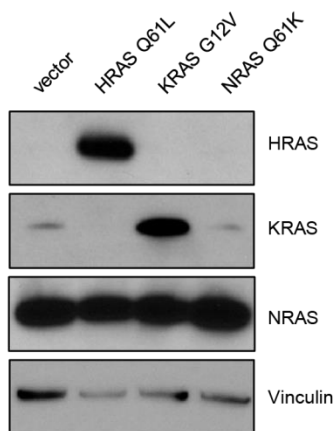
E



F



G



H

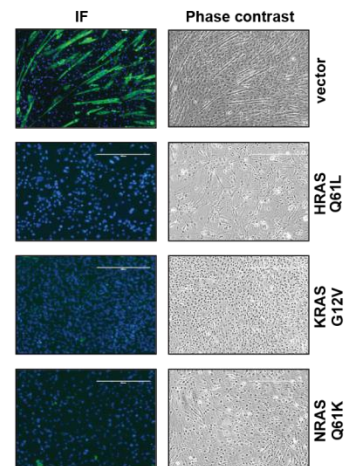


Fig. S3. ERK2 is associated with developmental gene regulation in RAS-mutated cancer cell lines. (A) Promoter proximal (<2500 bp from nearest transcriptional start site, green) and distal (enhancers, gray) ERK2 peaks are displayed as a dot plot. (B) GREAT analysis (top) shows that ERK2 peaks in SK-N-AS are enriched for pathways important for neural crest development (top). HOMER analysis reveals that these ERK2 peaks are enriched with binding motifs for AP-1 transcription factors (bottom). (C) Changes in H3K27ac deposition at the *MYOG* locus during skeletal muscle myogenesis. Data were accessed from the WashU Epigenome browser <http://epigenomegateway.wustl.edu>. (D) (top) Gene browser view of RNA Pol II ChIP-seq for SMS-CTR treated with DMSO or trametinib. In these figures, promoter density (-800 to -30 bp) is colored blue, transcriptional start site density (TSSR, -30 to +300 bp) is colored red, gene body density is colored purple and all other regions are green. (bottom) Pausing index and promoter stalling index calculations. (E) Scatter plots comparing pausing index (top) and promoter stalling index (bottom) genome-wide in SMS-CTR treated with DMSO or trametinib, highlighting that the change in *MYOG* promoter stalling index upon trametinib treatment is an outlier, whereas the change in *MYOG* pausing index is not. (F) RT-qPCR for *MYOG* expression in SMS-CTR cells treated for 6 hours with either 100 nM trametinib, 100 nM THZ1, an inhibitor of CDK7, 500 nM flavopiridol, an inhibitor of CDK9, or the indicated combinations of drugs. Data are represented as mean \pm SEM for 3 independent experiments. * denotes $p < 0.05$, as determined by unpaired t-test with Welch's correction. (G) Stable expression of RAS isoforms in C2C12 cells is confirmed by immunoblot. (H) Expression of oncogenic RAS isoforms (*HRAS* Q61L, *KRAS* G12V, or *NRAS* Q61K) prevents myogenic differentiation in C2C12 mouse myoblasts (left), as determined by a 5-day differentiation assay followed by immunofluorescence detection of myosin heavy chain (MHC, green) and phase contrast microscopy (right). Scale bars correspond to 400 μ m.

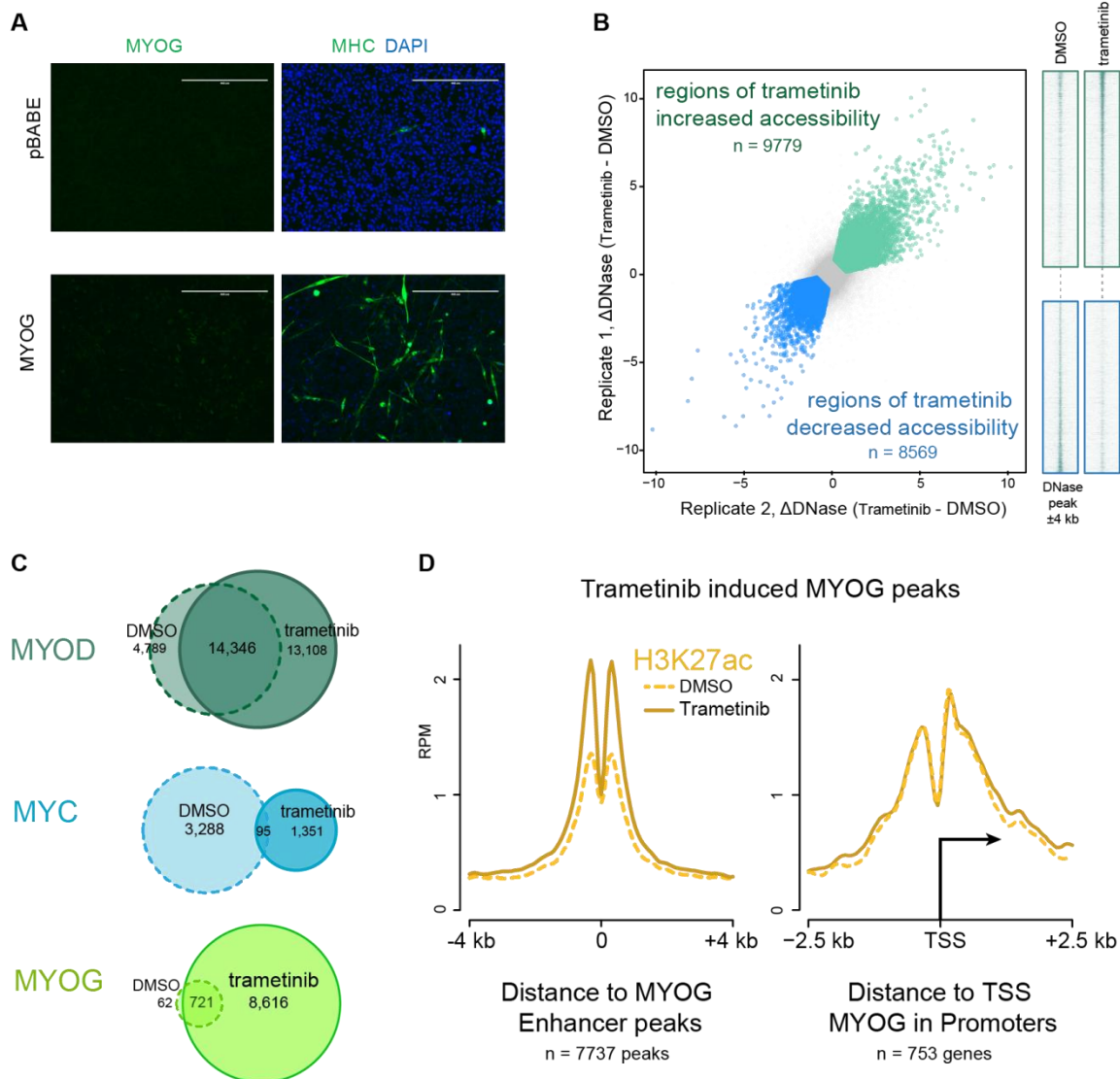


Fig. S4. MYOG associates with opened chromatin in trametinib-treated RMS cells. (A) Expression of MYOG (left) induces differentiation in RD, as determined by induction of MHC expression. Scale bars indicate 400 μ m. **(B)** Scatter plot comparing changes in DNase hypersensitivity reads genome-wide after 48 hours of trametinib treatment in SMS-CTR between two biological replicates. Regions of increased (aqua) and decreased (blue) accessibility due to trametinib treatment are indicated. DNase peak intensity in these regions is also shown in the heatmaps at right, in which each row represents a genomic location. The rows are centered around the peak of DNase hypersensitivity, extended 4kb in either direction, and sorted top to bottom by DNase peak intensity. **(C)** Venn diagrams depicting overlap between MYOD, MYC, and MYOG binding sites in DMSO and trametinib treated SMS-CTR. **(D)** Composite plots showing H3K27ac signal intensities (RPM) at trametinib-induced MYOG peaks found in enhancers (left) and promoters (right).

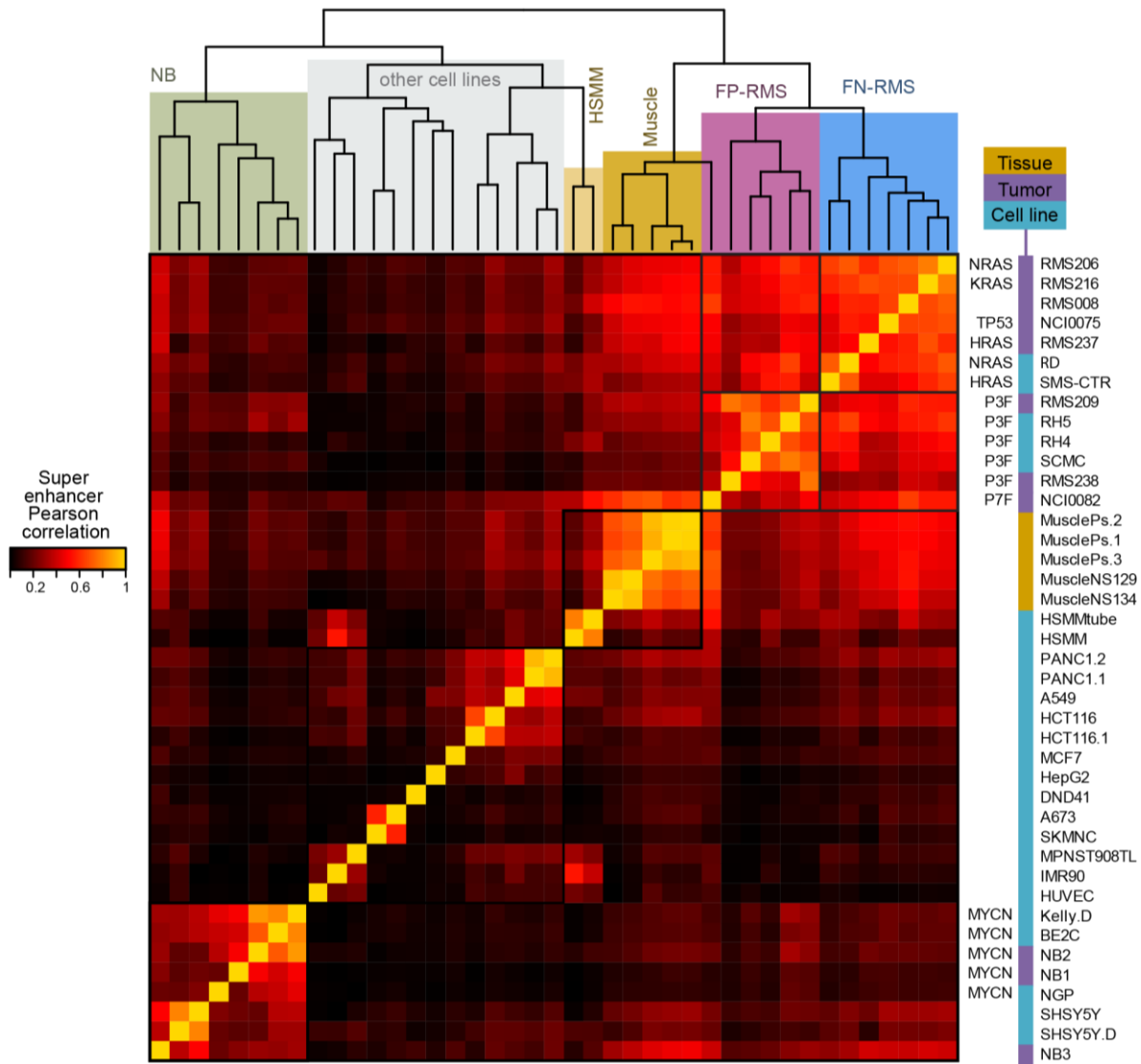


Fig. S5. Super-enhancers in RAS-mutated RMS cell lines correlate with super-enhancers in RAS-mutated RMS tumors. Correlation heatmap of super enhancers observed in FN-RMS cell lines and tumors (blue), FP-RMS cell lines and tumors (purple), normal skeletal muscle (gold), neuroblastoma cell lines (green), and other cancer patient-derived cell lines (gray). A strong positive correlation is indicated by a gold color on the heatmap, while no correlation is indicated by a black color. The dendrogram derived from the correlation is shown at the top of the heatmap. The cell lines (aqua), tumors (purple), and tissues used in this analysis are shown at right, as well as the driver somatic mutations.

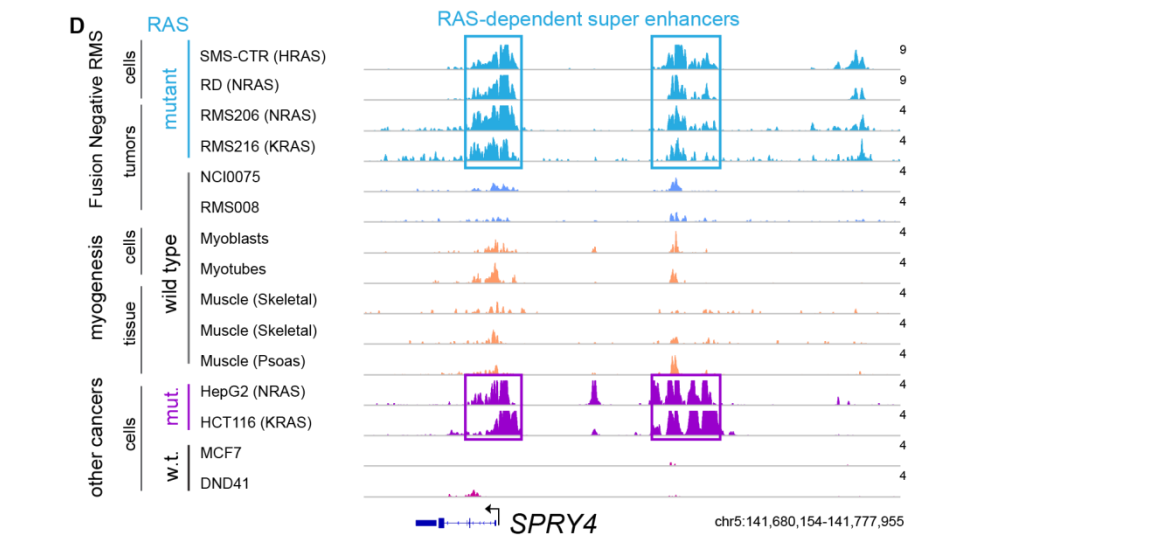
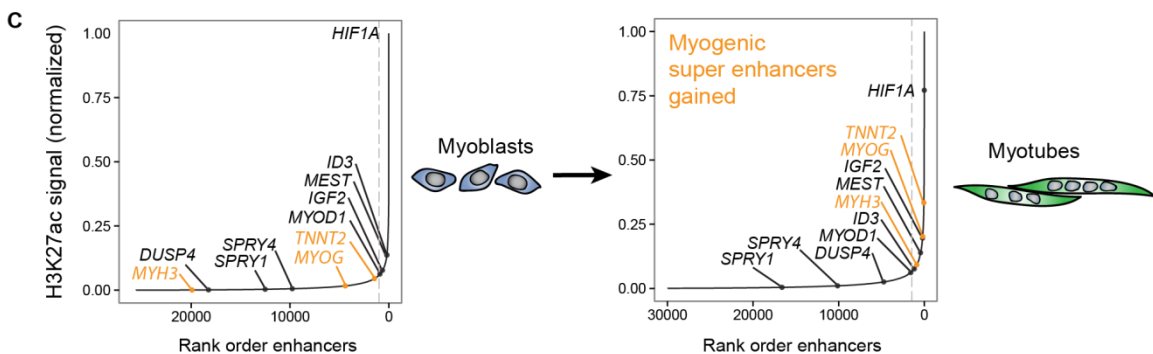
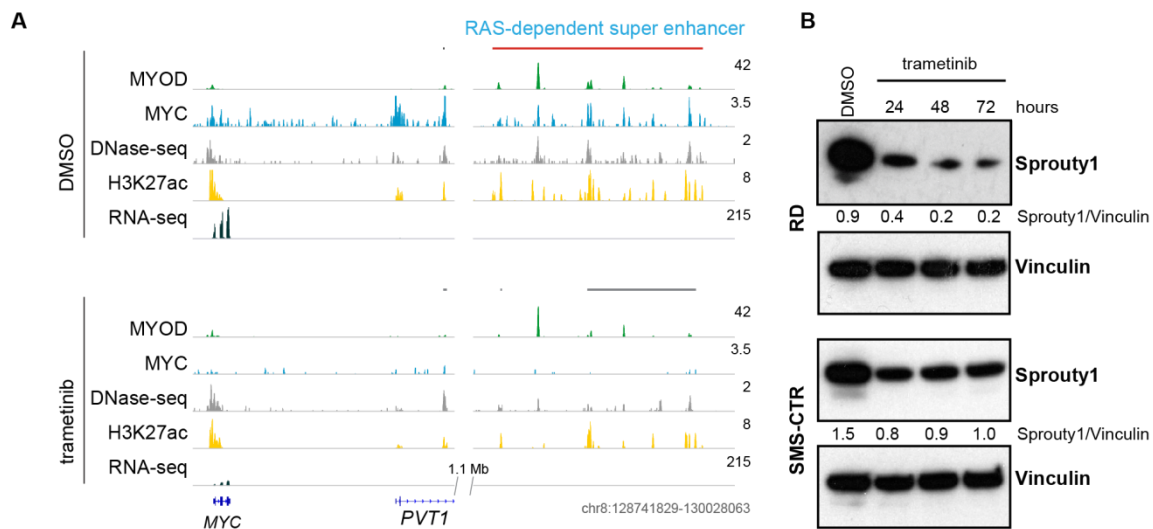


Fig. S6. RAS-dependent super-enhancers are not observed in human skeletal muscle myoblasts. (A) Signal tracks for *MYOD* (aqua), *MYC* (blue), and H3K27ac (yellow) ChIP-seq, DNase-seq (gray), and RNA-seq (dark green) experiments performed at the *MYC* locus on SMS-CTR treated with DMSO or trametinib for 48 hours. Predicted typical enhancers are shown above the signal tracks in gray; super-enhancers are red. (B) Expression of *Sprouty1* is decreased by trametinib treatment in RD and SMS-CTR, as determined by immunoblot. (C) Ranked order of H3K27ac-loaded enhancers in HSMM grown in complete medium (left) or differentiation medium (right) reveals super enhancers that are gained (gold) or unchanged (black) because of differentiation. (D) Signal tracks for H3K27ac at the *SPRY4* locus for FN-RMS cell lines (RD and SMS-CTR) and tumors (RMS206, RMS216, NCI0075, and RMS008, blue); normal skeletal muscle myoblasts, myotubes, and mature skeletal muscle (orange); RAS-mutated human cancer cell lines (purple); and RAS-wild type human cancer cell lines (red). Super-enhancers are indicated with boxes. Cell lines and tumors with RAS mutations are indicated.

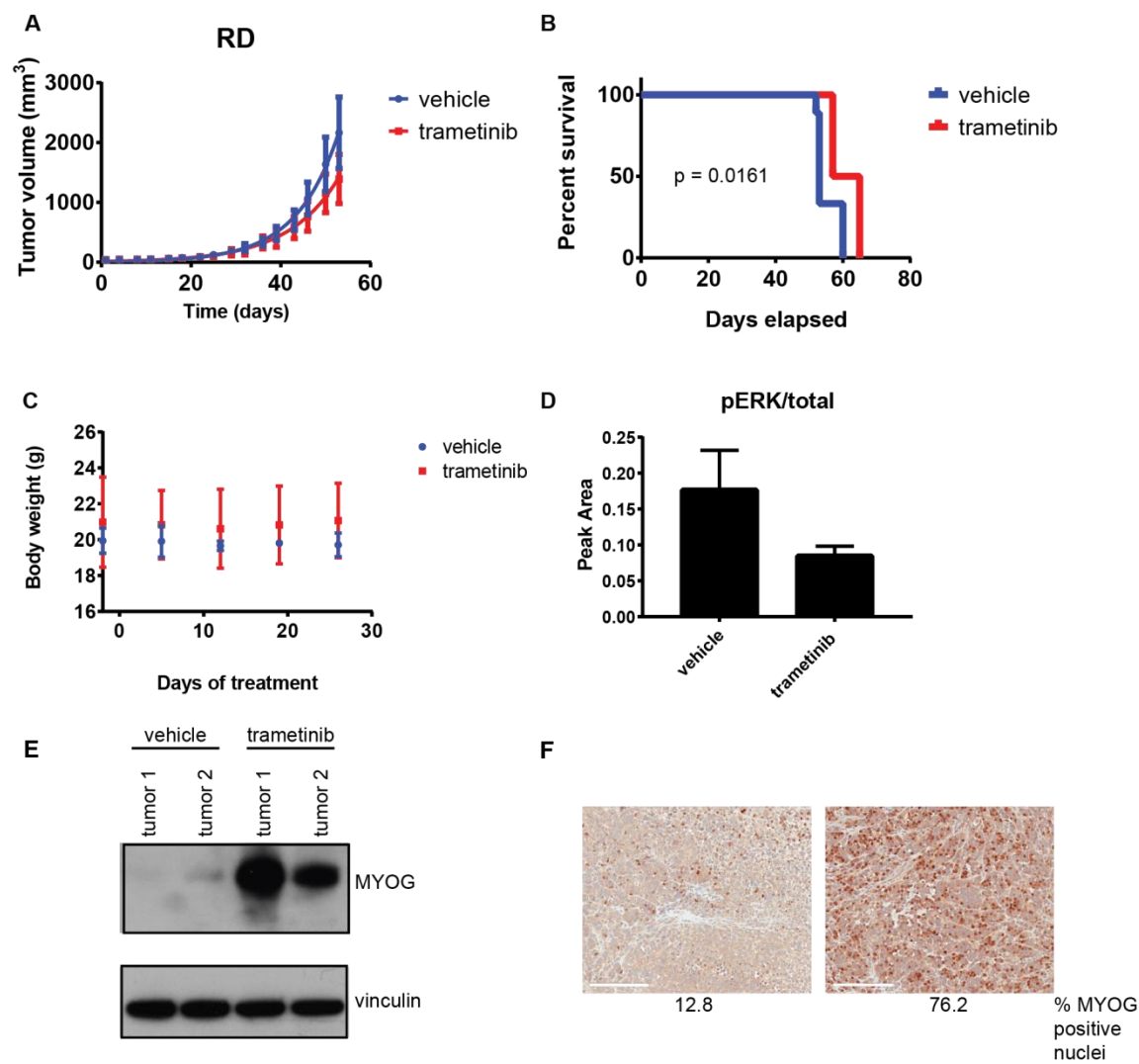


Fig. S7. MEK inhibition delays tumor growth in RD xenografts. (A) Daily trametinib treatment inhibits tumor growth in SCID Beige mice injected orthotopically with RD cells. * denotes $p < 0.05$ and ** denotes $p < 0.01$, unpaired t-test. (B) Daily trametinib treatment modestly but significantly prolongs overall survival in SCID Beige mice injected orthotopically with RD cells, p-value determined by log-rank test. (C) Daily trametinib did not cause weight loss in SCID Beige mice (RD, SMS-CTR and BIRCH models). (D) Trametinib treatment decreases ERK phosphorylation by 50% in RD xenografts as determined by capillary immunoassay. (E) Trametinib treatment increases *MYOG* expression in RD xenografts as determined by immunoblot and immunohistochemistry (F). Scale bars correspond to 200 μm .

Figure S8

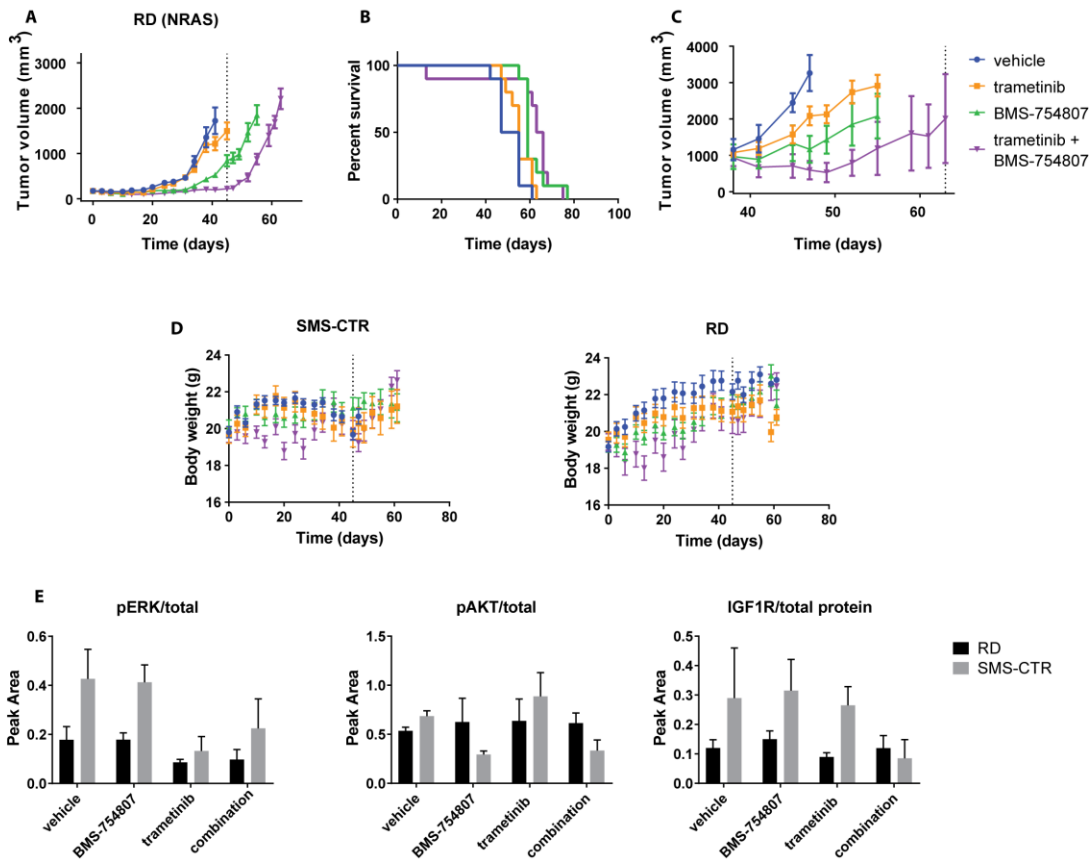


Fig. S8. Combination of trametinib and BMS-754807 delays tumor growth in RD xenografts. Daily treatment with the combination of trametinib and BMS-754807 prolongs the time to tumor development (A) and but does not prolong survival (B) in RD xenografts compared to BMS-754807 alone (p-value = 0.2881, Mantel-Cox test for the comparison between BMS-754807 and the combination). Dashed line indicates date at which treatment was stopped (45 days). (C) Daily treatment with the combination of trametinib and BMS-754807 stabilizes large tumors in RD xenografts. (D) Average weight for mice with SMS-CTR (left) or RD (right) xenografts receiving vehicle (blue), trametinib (orange), BMS-754807 (green) or the combination (purple). (E) Peak area of the ratio of phosphorylated to total ERK (top) and S473 AKT (middle) as determined by Simple Western is displayed for RD (black) and SMS-CTR (gray) xenografts treated with vehicle, trametinib, BMS-754807 or the combination for 5 days. Also depicted is the ratio of total IGF1R to total protein as determined by Simple Western. Vehicle and trametinib pERK/total ratios are represented from Fig. 6B (SMS-CTR) and s7E (RD) for comparison.

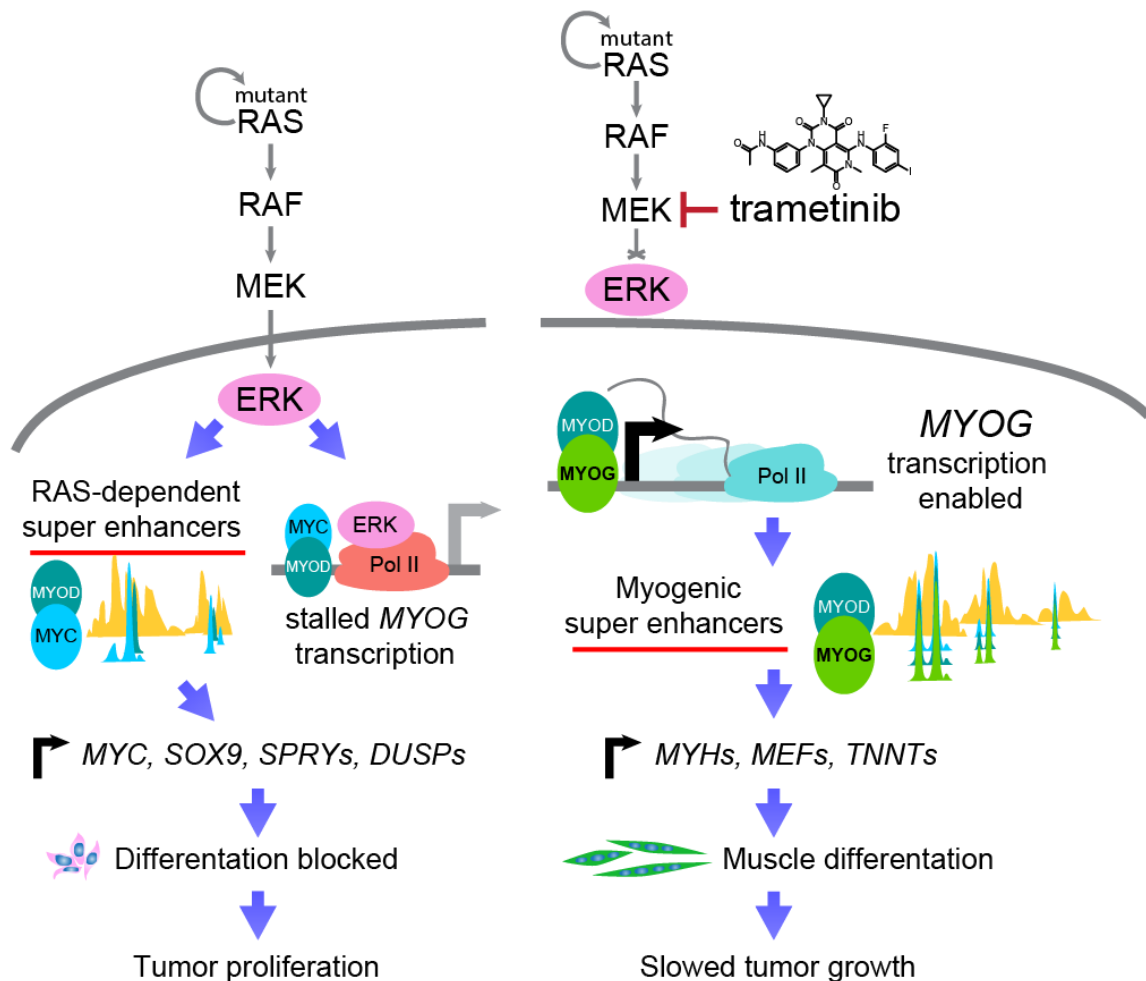


Fig. S9. MEK inhibition induces transcriptional reprogramming analogous to myogenic differentiation in FN-RMS. (left) In the absence of trametinib, oncogenic RAS isoforms induce aberrant MAP kinase signaling, which contributes to maintenance of proliferation and self-renewal as well as a block in myogenic differentiation in FN-RMS. Maintenance of proliferation is achieved in part through the establishment of RAS-dependent super-enhancers at loci of genes that play a role in cellular proliferation (*MYC*, *SOX9*, *SPRYs*, *DUSPs*). The differentiation block is mediated through the binding of ERK2 to the *MYOG* locus, stalling RNA Pol II entry into the TSS of that gene. In RAS-driven RMS, the combination of the maintenance of cellular proliferation and the block in differentiation allows tumor growth. (right) MEK inhibition with trametinib in FN-RMS releases *MYOG* expression from ERK-dependent suppression, allowing *MYOG* to activate genes important for myogenic differentiation (*MYHs*, *MEFs*, *TNNTs*) by inducing chromatin remodeling and establishment of super-enhancers. In RAS-driven RMS, this induction of muscle differentiation slows tumor growth.